NASA/TM—2013-217874

AIAA–2013–1619

Quantifying Effects of Voids in Woven Ceramic Matrix Composites

Marlana B. Goldsmith, Bhavani V. Sankar, and Raphael T. Haftka
University of Florida, Gainesville, Florida

Robert K. Goldberg
Glenn Research Center, Cleveland, Ohio

June 2013

NASA STI Program . . . in Profile

Since its founding, NASA has been dedicated to the advancement of aeronautics and space science. The NASA Scientific and Technical Information (STI) program plays a key part in helping NASA maintain this important role.

The NASA STI Program operates under the auspices of the Agency Chief Information Officer. It collects, organizes, provides for archiving, and disseminates NASA's STI. The NASA STI program provides access to the NASA Aeronautics and Space Database and its public interface, the NASA Technical Reports Server, thus providing one of the largest collections of aeronautical and space science STI in the world. Results are published in both non-NASA channels and by NASA in the NASA STI Report Series, which includes the following report types:

- TECHNICAL PUBLICATION. Reports of completed research or a major significant phase of research that present the results of NASA programs and include extensive data or theoretical analysis. Includes compilations of significant scientific and technical data and information deemed to be of continuing reference value. NASA counterpart of peer-reviewed formal professional papers but has less stringent limitations on manuscript length and extent of graphic presentations.

- TECHNICAL MEMORANDUM. Scientific and technical findings that are preliminary or of specialized interest, e.g., quick release reports, working papers, and bibliographies that contain minimal annotation. Does not contain extensive analysis.

- CONTRACTOR REPORT. Scientific and technical findings by NASA-sponsored contractors and grantees.

- CONFERENCE PUBLICATION. Collected papers from scientific and technical conferences, symposia, seminars, or other meetings sponsored or cosponsored by NASA.

- SPECIAL PUBLICATION. Scientific, technical, or historical information from NASA programs, projects, and missions, often concerned with subjects having substantial public interest.

- TECHNICAL TRANSLATION. English-language translations of foreign scientific and technical material pertinent to NASA's mission.

Specialized services also include creating custom thesauri, building customized databases, organizing and publishing research results.

For more information about the NASA STI program, see the following:

- Access the NASA STI program home page at *http://www.sti.nasa.gov*

- E-mail your question to *help@sti.nasa.gov*

- Fax your question to the NASA STI Information Desk at 443–757–5803

- Phone the NASA STI Information Desk at 443–757–5802

- Write to:
  STI Information Desk
  NASA Center for AeroSpace Information
  7115 Standard Drive
  Hanover, MD 21076–1320

Quantifying Effects of Voids in Woven Ceramic Matrix Composites

Marlana B. Goldsmith, Bhavani V. Sankar, and Raphael T. Haftka
University of Florida, Gainesville, Florida

Robert K. Goldberg
Glenn Research Center, Cleveland, Ohio

National Aeronautics and
Space Administration

Glenn Research Center
Cleveland, Ohio 44135

Acknowledgments

Level of Review: This material has been technically reviewed by technical management.

Available from

Quantifying Effects of Voids in Woven Ceramic Matrix Composites

Marlana B. Goldsmith, Bhavani V. Sankar, and Raphael T. Haftka
University of Florida
Gainesville, Florida 32611

Robert K. Goldberg
National Aeronautics and Space Administration
Glenn Research Center
Cleveland, Ohio 44135

Abstract

Randomness in woven ceramic matrix composite architecture has been found to cause large variability in stiffness and strength. The inherent voids are an aspect of the architecture that may cause a significant portion of the variability. A study is undertaken to investigate the effects of many voids of random sizes and distributions. Response surface approximations were formulated based on void parameters such as area and length fractions to provide an estimate of the effective stiffness. Obtaining quantitative relationships between the properties of the voids and their effects on stiffness of ceramic matrix composites are of ultimate interest, but the exploratory study presented here starts by first modeling the effects of voids on an isotropic material. Several cases with varying void parameters were modeled which resulted in a large amount of variability of the transverse stiffness and out-of-plane shear stiffness. An investigation into a physical explanation for the stiffness degradation led to the observation that the voids need to be treated as an entity that reduces load bearing capabilities in a space larger than what the void directly occupies through a corrected length fraction or area fraction. This provides explanation as to why void volume fraction is not the only important factor to consider when computing loss of stiffness.

Nomenclature

a	Void area
A	FEA model area
C	Material stiffness matrix
E	Young's modulus
G	Shear modulus
l	Height of void
L	FEA model height
ξ	Height correction factor
V_v	Void volume fraction
ν	Poisson's ratio

1.0   Introduction

Aircraft and spacecraft components that undergo extreme thermo-structural loads have reached some material limitations in terms of strength and weight. Woven ceramic matrix composites (CMCs), in particular, are candidate materials for future hypersonic vehicle components such as thermal protection and aero-propulsion systems due to their high strength and fracture toughness at elevated temperatures

(Ref. 1). However, variability in the stiffness and strength may limit widespread implementation. Some of the variability is believed to be due to randomness in the architecture (tow spacing, tow size, tow nesting), as well as the unevenly shaped and spaced voids created as a result of the randomness in architecture and the nature of the manufacturing process. Variability also exists in the material properties of the constituents, but its effects on stiffness and strength are thought to be smaller than the variability due to architectural randomness.

Recent work completed by the authors found that variation in tow size and tow spacing alone does not explain all of the variability found in the stiffness of the ceramic matrix composite system under investigation (Ref. 2). Instead, we hypothesized that the variable size and spacing of the voids plays a larger role in the variability of the composite properties. The effects of voids have been studied in the past with a variety of methods and goals. There is a large body of work in which the results are related mostly to void volume fraction (Refs. 3 to 6). The relationships found may be relevant for some applications, but as will be shown later, the volume fraction of the voids is not the only thing that must be considered in the woven ceramic matrix composite under consideration in this work. The voids considered here are unevenly distributed and many have large aspect ratios. Others have shown the importance of the microstructure including Tsukrov and Kachanov (Ref. 7) who accounted for elliptical voids with arbitrary orientations and eccentricities. This work is limited to a 2D anisotropic solid and the holes are non-interacting. Huang and Talreja (Ref. 8) demonstrated that the void shape and size was an important factor to consider, especially for transverse and shear stiffness of a unidirectional composite. They also observed that long, flat voids are most detrimental to the transverse stiffness. This agrees well with preliminary analysis on the woven Chemical Vapor Infiltration (CVI) SiC/SiC composite where void volume fraction is not the sole mechanism of stiffness degradation (Ref. 9). Uniform distribution of voids was assumed for the analysis which was shown to compare well for experimental data in unidirectional composites. However, woven composites appear to have significantly greater variability in void size and distribution as compared to unidirectional composites.

The previous work on the effects of voids as discussed above provides insight into some of the mechanisms that contribute to stiffness degradation, and provide a benchmark to which observations in this paper can be qualitatively compared. However, the intent of the current work is to be able to use quantitative information about randomly spaced and shaped voids to make quantitative predictions of the resulting stiffness. The motivation and background for this work is provided in Section 2.0. The investigation begins with using finite element analysis to study the effects of non-overlapping voids (aligned in one plane) in an isotropic material, rather than a composite, so that the results are not convoluted by the other architectural variants. As will be demonstrated below, this is a good assumption to begin with since the variability in stiffness due to other architectural variations such as tow size and tow spacing contribute a relatively small amount to the variability in stiffness. Once the physical mechanisms of the effects of voids are understood at this level, the procedures can be extended to understand more complex material systems such as a composite.

2.0   Characterization of Composite Variability

The composite system under investigation is a CVI SiC/SiC eight ply 5HS (harness satin) weave material. The composite has continuous Sylramic-iBN fiber tows (20 ends per inch) woven into a five-harness woven fabric preform in a [0°/90°] pattern. A silicon-doped boron nitride coating is deposited on the surface of the individual fibers in the tows. The fiber preform is then infiltrated with a CVI-SiC matrix which fills the tows and forms a thin matrix coating around the tows. The constituent material properties can be found in Reference 9. A 2D image of one cross section of the SiC/SiC composite, obtained by Goldberg, Bonacuse, and Mital is shown in Figure 1 (Ref. 9). The black areas in the interior of the cross section represent voids (the black area comprising the border of the image is not voids), which vary in location, size, and shape. Other 2D cross sections exhibit different random distributions of the voids and the architectural characteristics such as tow size, shape, and spacing.

Finite element analysis of three cross sections similar to that of Figure 1 revealed significant variability in the transverse modulus (E_3) that did not correlate to constituent volume fractions (VF), as shown in Table 1 (Ref. 9). Note that E_1 is the modulus in the longitudinal direction as labeled by the coordinate system in Figure 1. This will be referred to as the in-plane modulus. Since the composite is stacked in a [0°/90°] pattern, E_1 is assume to be equal to E_2 E_3 will be referred to as the transverse, or out-of-plane, modulus.

In an attempt to capture the variability, finite element analysis based micromechanics and monte carlo simulations were used to analyze a large number of hypothetical cross sections (modeled as representative volume elements (RVEs)) that were generated based on quantified variability found in the tow width, tow height, and tow spacing. A typical RVE is represented in Figure 2. It consists of two stacked unit cells that are offset from one another by the width of one tow. This ply shifting of one tow offset was held constant for all RVEs with varying tow parameters. The results generated are summarized in Table 2, and they indicate that the architectural parameters that were varied were not enough to capture the variability exhibited by the full cross sections. In addition, the stiffnesses were correlated mostly to the volume fractions of the constituents which we know is not entirely the case. Details of the analysis can be found in Reference 2.
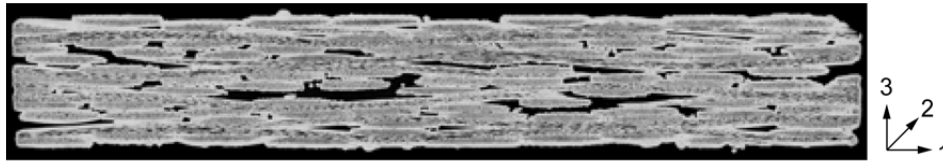

Figure 1.—2D cross section of the SiC/SiC composite microstructure (Ref. 9).

TABLE 1.—FEA RESULTS OF MODULI FOR FULL CROSS SECTIONS

	Void VF	Tow VF	Matrix VF	E_1	E_3
Cross section 1	3.2	63.0	33.8	237	103
Cross section 2	4.8	62.8	32.4	227	77
Cross section 3	3.5	63.9	32.6	234	51

Figure 2.—Example of a randomly generated RVE.

TABLE 2.—STATISTICAL PROPERTIES OF MODULI
FROM MONTE CARLO SIMULATIONS
OF RVE ANALYSIS

	Mean	Standard deviation
E_1 (GPa)	231.0	5.0
E_3 (GPa)	105.8	6.2

As previously mentioned, one major component of the architectural variation not considered in the RVE analysis was ply shifting since it could not be quantified in the same manner as the tow size and spacing. An investigation into the effects of ply shifting indicated that it significantly affected the variability of the stiffness, as shown in Table 3. The results shown are for one RVE (tow size and spacing remains constant), with varying tow offsets. The magnitude of the tow offset is defined by assuming perfectly aligned tows or unit cells initially, then prescribing one unit cell to be offset by a certain fraction of a tow width. The variation in the shifting affects the out-of-plane modulus significantly. This effect is mostly due to rearrangement of macroscopic voids. The variability in ply shifting decreases the average value of the modulus and increases the amount of variability as compared to the results in Table 2.

A visual assessment of the voids in Figures 3 to 5 provides clarity into the increased variability in the moduli due to shifting. It is known that voids have a significantly more detrimental effect on the out of plane moduli than the in-plane moduli for varying void content as well as for flat shapes (Ref. 8). The RVE with the tow offset of one tow has one void with a large aspect ratio, and several that are square in shape. The cross section in Figure 5 has several voids with large aspect ratios distributed throughout the composite, which is better represented by the RVE in Figure 4. As previously mentioned, the work of Huang and Talreja (Ref. 8) emphasize the importance of considering the size and aspect ratio of the voids. Clearly, when there are more voids with large aspect ratios the stiffness is significantly reduced.

TABLE 3.—MODULI FOR ONE RVE
DUE TO SHIFTING VARIATION
(FIGS. 3 AND 4)

Shifting (tow offset)	E_1	E_3
1.00 (current RVE)	224	106
0.75	221	92
2.50	231	82
3.25	234	89
4.50	218	70

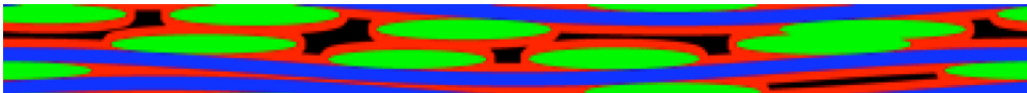Figure 3.—RVE with tow offset equal to 1.0.
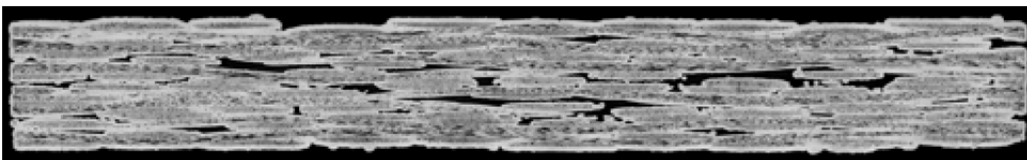

Figure 4.—RVE with tow offset equal to 4.5.

Figure 5.—Cross section 2.

3.0   Analysis Methods

With each new ply shifting applied, the key architectural change is the size, shape, and location of the voids. Some qualitative effects have been studied, but it would be useful to have predictive models to estimate the mechanical properties, as well as to provide a physical understanding. The microstructure of the 5HS SiC/SiC composite is very complicated. In order to develop an understanding of the effects of voids, without the results being convoluted by other aspects of the material geometry, the preliminary analysis will be completed on an isotropic material with a Young's modulus of 100 GPa and a Poisson's ratio of 0.3.

3.1   Finite Element Model

Previous analysis of the effects of tow variability was completed in 2D for simplicity. This is not the best way to model the woven composite, but it gives reasonable estimates in regard to modeling the variability. Since modeling the variability in the tow size and tow spacing led to relatively small variability in the stiffness, it may be possible to capture the variability in the composite specimens by modeling only the voids, and not the other details of the microstructure. At the least, studying the effects of voids in an isotropic material will provide valuable preliminary insight into the physical effects of voids on the composite. This also simplifies the problem so that the effects of voids can be studied in 3D, eliminating some of the shortcomings of a 2D approximation, especially when considering the shear stiffness.

Finite element analysis was completed using Abaqus (Ref. 10), with 4-node tetrahedron elements. Periodic boundary conditions were applied such that one of the macro strains was non-zero and all other strains and the temperature differential ΔT were zero. The macro-stresses were calculated by averaging the micro-stresses in the RVE. Using the six macro-stresses one can determine the first column of the stiffness matrix, C. The procedure was repeated for the other five macro stains to calculate the entire C matrix. From C one can calculate the elastic constants using the relations of the type shown in Equation (1) where C is the

$$[C]^{-1} = [S] = \begin{bmatrix} S_{11} & ... & S_{16} \\ ... & ... & S_{26} \\ S_{61} & ... & S_{66} \end{bmatrix}_{(6\times6)} \tag{1}$$

$$S_{11} = \frac{1}{E_1}, S_{12} = \frac{v_{21}}{E_2}, S_{66} = \frac{1}{G_{12}}, \text{etc.}$$

material stiffness matrix, S is the material compliance matrix, v is Poisson's ratio, and E and G are Young's moduli and shear moduli, respectively.

The finite element model depicted in Figure 6 is a cuboid of equivalent length and width. The aspect ratio (ratio of the length to the height) is 4 to 1, similar to that of the composite cross sections that were
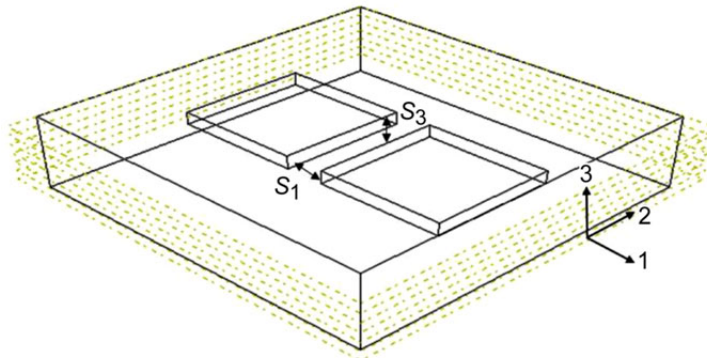

Figure 6.—3D model with 2 cuboid voids.

available. The voids were modeled as cuboids. The sharp corners do not affect the stiffness results; however they will be avoided if a similar model is used for examining the effects of voids on strength. The length and width of a given void are also equivalent. Since the composite's weave is balanced, it is safe to assume that if the voids are of a given length when scanning from the 1-3 plane, they will be similar when scanning from the 2-3 plane. The voids can occur anywhere in the 1-2 plane. However, the location on the 3-axis is constrained to 7 different layers. This reflects the fact that the voids generally occur in the interlaminar positions, or between the plies. The descriptions of the specific void sizes and locations studied are given in the following section.

3.2   Description of Void Cases

The variables for this study are the number of voids, the aspect ratio, and the position of the voids. The aspect ratio (AR) is defined by the width (1-direction) divided by the height (3-direction). The size (8 by 8 by 2 mm) and isotropic material properties of the specimen will remain constant, in addition to the total void volume fraction of 4 percent. The specimen itself has an aspect ratio of 4. The initial exploratory results encompass 20 cases summarized pictorially in Figures 7 to 12. Additional 1-void cases in which the length did not equal the width were analyzed for the shear stiffness analysis.
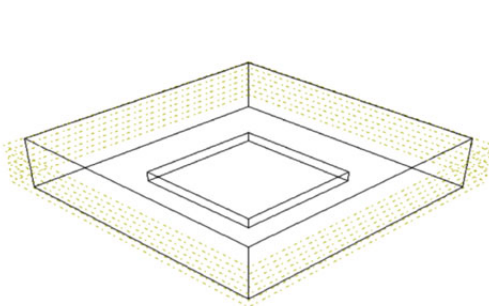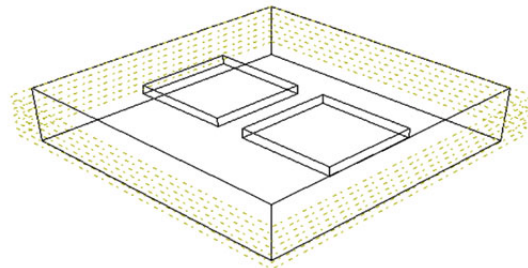
Figure 7.—1 Void; centered; varying AR.

Figure 8.—2 Voids; centered along 1-axis; varying AR, S_1, and S_3.
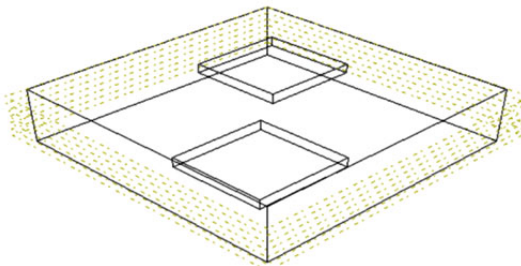
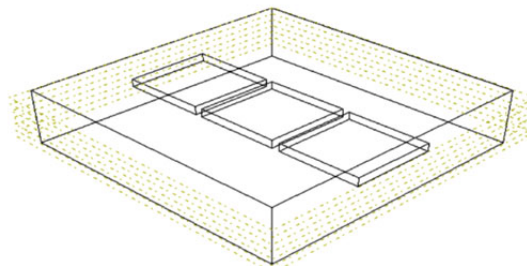Figure 9.—2 Voids; AR = 8; voids in opposite corner.

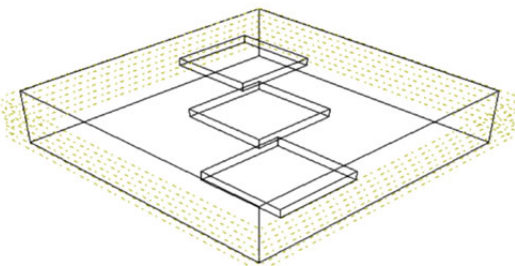Figure 10.—3 Voids; centered; varying AR.

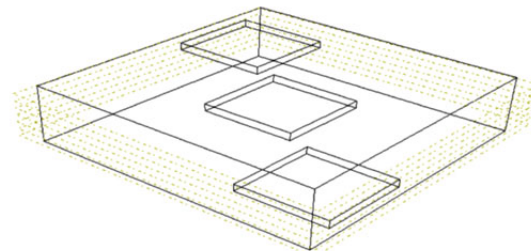Figure 11.—3 Voids; arranged diagonally on one plane.

Figure 12.—3 Voids; arranged diagonally on multiple planes.

A more thorough description of each case and the FEA results relating to them can be found in Tables A.1 and A.2. The variables include the number of voids, the aspect ratio of the voids (aspect ratio of length to height, since length and width are assume to equivalent), and the position of the voids. Some positions are not surveyed due to symmetry.

4.0   Results and Analysis

After analyzing 20 exploratory void cases, a few trends became obvious. The longitudinal stiffness and in-plane shear stiffness were not significantly affected by changes in the void aspect ratio and location. However, the transverse stiffness and out-of-plane shear stiffness were significantly affected. For a constant void volume fraction of 4.0 percent, the loss in stiffness averaged up to 15 percent. This is significant in that many models accounting for voids rely on void volume fraction alone. For the particular composite studied here, there are other factors besides volume fraction that must be significant and important to consider. The average loss of stiffness and the respective standard deviation is displayed in Table 4. When considering the effects of placing the voids in various locations with respect to one another, the stiffness is minimally impacted. This may not be true for cases in which voids are overlapping which will be explored in future work.

TABLE 4.—LOSS OF STIFFNESS BASED ON 20 VOID CASES WITH A CONSTANT
VOLUME FRACTION OF 4.0 PERCENT, DESCRIBED IN
SECTION 3.0 AND THE APPENDIX

	E_1	E_2	E_3	G_{12}	G_{13}	G_{23}
Average percent loss of stiffness	0.7	1.0	12.5	1.2	12.4	14.9
Standard deviation	0.5	0.5	4.1	0.7	3.1	4.4

4.1   Transverse Stiffness Analysis and Results

The remaining results and analysis shown in this paper will consider the transverse stiffness and shear stiffness. When examining the results of the transverse stiffness, there is an obvious pattern that shows that as the aspect ratio of the void increases, the stiffness decreases. The key feature of the void that is changing as the aspect ratio increases, is the area of the void on the 1-2 plane. It became clear that the projected area of the voids in the transverse direction (or the area of the void in the 1-2 plane) was important to determining the stiffness. The plot in Figure 13 plots the transverse stiffness as a function of the area fraction, $\bar{a}_3$, which can be define as the ratio of the projected void area, a_3, to the total area of the 12 plane, A_3, and written as

$$\bar{a}_3 = \frac{a_3}{A_3} \tag{2}$$

A strong linear relationship is found between the projected area of the voids and the resulting stiffness. The equation of the line is

$$E_3 = -70.96\bar{a}_3 + 102.79 \tag{3}$$

and the coefficient of determination, R^2, is 0.98. There is obviously a small error in the fit because we know that the intercept should be 100 (at a void ratio of 0, the stiffness should be 100 GPa). Using the linear equation, the void cases not used for the fit (cases with various void spacing) can be used to check how well the fit predicts the stiffness for other void cases. When using the equation, the RMS (root mean square) error was 0.45 GPa which is very small. Using the equation does not account for any variability due to spacing, since the area ratio is the only input. It is important to note again that the voids' placement did not significantly affect the stiffness, so the relative variability in that data set is small.
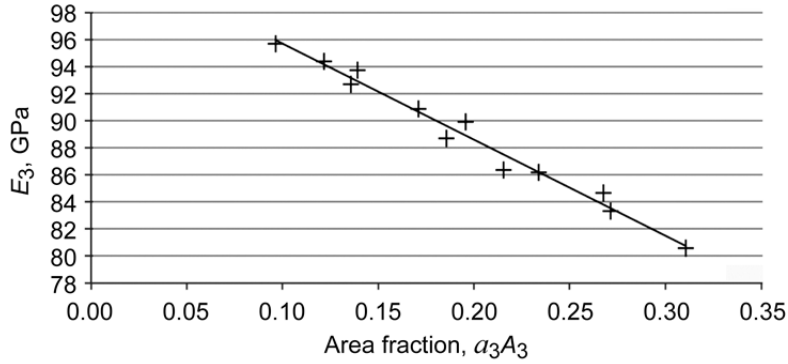
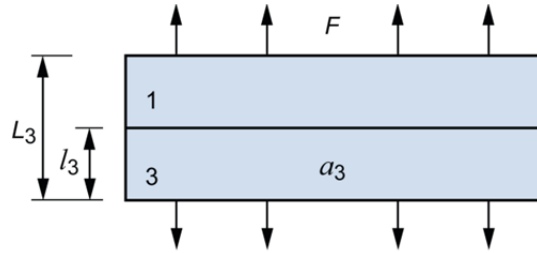Figure 13.—Plot of area ratio versus resultant transverse stiffness.

Figure 14.—Illustration of example problem.

The relationship of the projected area to the transverse stiffness may be useful, but it does not provide any physical understanding about the effects of voids. Intuitively one would assume the slope of the line in Figure 13 would be –100, which is not the case. In order to arrive at a physical explanation we can examine a problem in which we have two materials stacked on top of one another as shown in Figure 14. The displacement of the material can be written as

$$\Delta_3 = \frac{F(L_3 - l_3)}{A_3 E_3} + \frac{F l_3}{(A_3 - a_3) E_3} = \frac{F L_3}{A_3 E'_3} \tag{4}$$

where F is a force applied to the material, A_3 is the area of the material, a_3 is the area of the void in Material 3, L_3 is the total length of the isotropic material in the 3-direction, l_3 is the length of the void, E_3 is the material's nominal stiffness, and E'_3 is the resultant stiffness due to the void. A 3D image is provided in Figure 15.

Equation (4) simplifies to

$$\frac{1}{1 - \dfrac{\Delta E_3}{E_3}} = 1 + V_v \frac{1}{(1 - \bar{a}_3)} \tag{5}$$

where V_v is the void volume fraction, ΔE_3 is the change in trasverse stiffness due to the voids, and $\bar{a}_3$ was defined in Equation (2). If $\bar{a}_3$ and $\dfrac{\Delta E_3}{E_3}$ are small, the following approximation can be used:
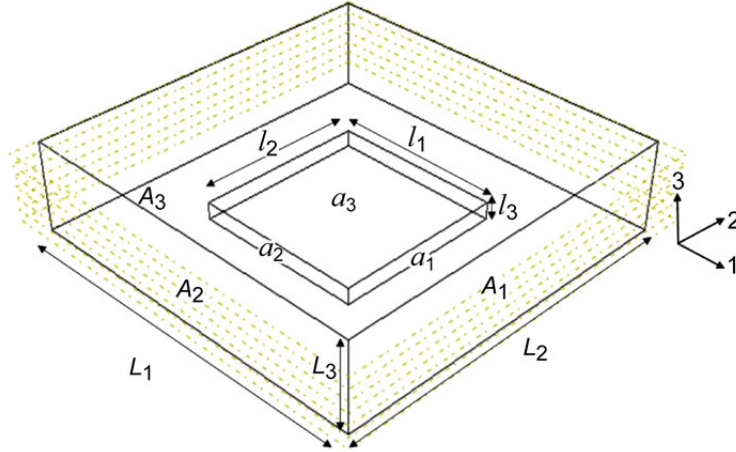
$$\frac{1}{1 - x} \approx 1 + x$$

Figure 15.—Definition of geometry.

Equation (5) then simplifies to

$$\frac{\Delta E_3}{E_3} = V_v \left(1 + \overline{a}_3\right)$$

(6)

This relationship poorly predicts the FEA result, with an RMS error of 8.2 GPa. It was hypothesized that the height of the void, l_3, has an effect on the stiffness that extends beyond the nominal height. Equation (6) can then be rewritten as

$$\frac{\Delta E_3}{E_3} = \overline{a}_3 \left(\overline{l}_3 + \xi\right)\left(1 + \overline{a}_3\right) = V_v \left(1 + \overline{a}_3\right) + \xi \overline{a}_3 \left(1 + \overline{a}_3\right)$$

(7)

where ξ is a correction factor to the height fraction of the void and $\overline{l}_3$ is the height fraction of the void

$$\overline{l}_3 = \frac{l_3}{L_3}$$

The height fraction may be referred to as the length fraction, also. In order to determine what the correction factor should be, the results from the basic approximation given by Equation (6) and the FEA results can be used to solve for ξ with the equation as derived below.

$$\frac{\Delta E_3^{FEA}}{E_3} - \frac{\Delta E_3^{analytical}}{E_3} = V_v \left(1 + \overline{a}_3\right) + \xi \overline{a}_3 \left(1 + \overline{a}_3\right) - V_v \left(1 + \overline{a}_3\right)$$

$$\xi = \frac{\dfrac{\Delta E_3^{FEA}}{E_3} - \dfrac{\Delta E_3^{analytical}}{E_3}}{\overline{a}_3 \left(1 + \overline{a}_3\right)}$$

(8)

When the values for ξ are solved and plotted against the original length fraction, $\bar{l}_3$, a strong linear relationship exists, shown in Figure 16. The effective length fraction, $\bar{l}'_3$, can also be plotted against the original length as shown in Figure 17 so that there is a relationship between the original length fraction and the effective length fraction.

$$\bar{l}'_3 = \bar{l}_3 + \xi \tag{9}$$

The relationship between the original length fraction and the corrected length fraction is

$$\bar{l}'_3 = -0.33\bar{l}_3 + 0.51 \tag{10}$$

The need for a corrected length implies that there is more material that is not load-bearing than simply the space of the void in the total RVE volume. Instead, it extends farther through the thickness. The 45° line on the graph of Figure 17 represents the result if no correction was applied (the length fraction is equal to the corrected length fraction). The line demonstrates a clear difference between the original length fraction and that of the corrected length fraction. As the original length of the void increases, the correction factor and thus the amount the length needs to be corrected decreases. This reflects the fact that as the void's size increases, its influence on the material around it is reaching the boundaries of the material and thus cannot be further corrected.
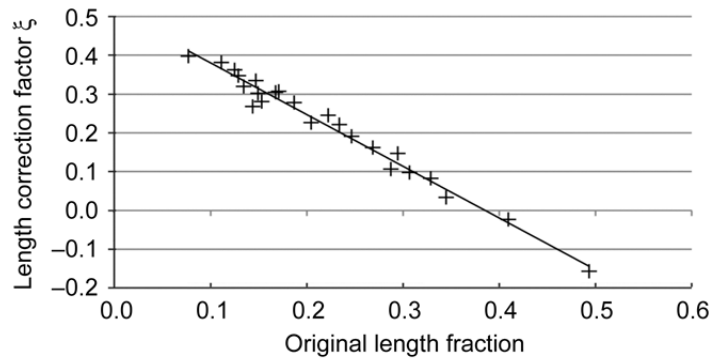

Figure 16.—Original length fraction $\bar{l}_3$ versus the length correction factor ξ.
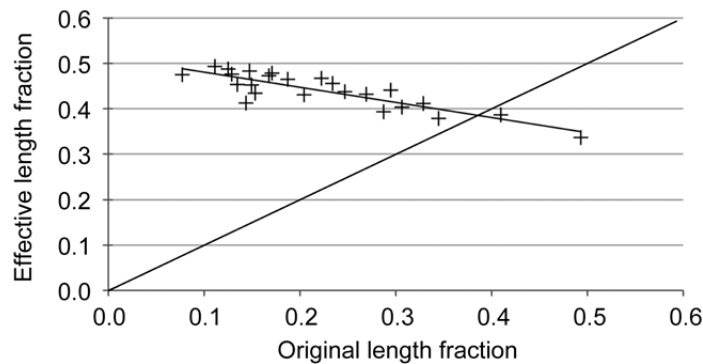

Figure 17.—Original length fraction $\bar{l}_3$ versus the effective length fraction $\bar{l}'_3$. The 45° line illustrating the difference between the original length fraction and the corrected value.

	ΔE_3 linear regression, GPa	ΔE_3 corrected equation, GPa	ΔE_3 FEA, GPa
1 void, AR = 3	4.1	4.8	6.3
1 void, AR = 5	6.8	6.4	7.3
1 void, AR = 8	10.4	9.7	11.3
1 void, AR = 10	12.5	11.8	13.7
2 voids, s_3 = max	13.8	13.2	14.0
4 voids, 4 different AR's, aligned	7.7	7.3	7.7

Table 5 provides a comparison of the predicted decrease in the transverse stiffness for a few sample cases using Equation (3), for linear regression to the projected area, and Equation (7), using the corrected length fraction, versus the results from FEA. Both methods appear to be reasonable at predicting the stiffness loss due to voids for the given cases.

5.0   Shear Stiffness Analysis and Results

The shear stiffness discussion presented here is based on analysis of only one void of varying size in order to more easily see the effects of the geometry of the void on the stiffness reduction. The shear stiffnesses as the area fraction of the void, $\bar{a}_3$, changes are plotted in Figure 18. For all data the height of the void, l_3, are held constant. Varying heights affected the stiffness by less than 5 percent. A quadratic relationship is found between the projected area of the voids and the resulting stiffness. The equation of the line is

$$G_{13} \approx G_{23} = -10.9\bar{a}_3{}^2 - 26.77\bar{a}_3 + 38.46 \qquad (11)$$

In the same way that the transverse stiffness calculation must account for a corrected length, the shear stiffness calculation must account for a corrected area. The shear stress at the wall of the void is zero, and small near the boundary of the void. In this way, the effect of the void on the stresses extends further than just the space the void occupies. This is illustrated in Figure 19. The equations below are derived with respect to G_{13}, but are written similarly for G_{23} also.

A similar relationship to that of Equation (5) can be derived for the shear stiffness reduction

$$\frac{1}{1 - \dfrac{\Delta G_{13}}{G_{13}}} = 1 + \frac{V_v}{(1 - \bar{a}_3)} = 1 + \frac{\bar{l}_3 \bar{a}_3}{1 - \bar{a}_3} \qquad (12)$$

Assuming a corrected area is necessary, a relationship between the corrected area $\bar{a}'_3$ and the calculated shear stiffness reduction according to finite element analysis can be written as

$$\bar{a}'_3 = \frac{\dfrac{\Delta G_{13}}{G_{13}}}{\dfrac{\Delta G_{13}}{G_{13}} - \dfrac{\Delta G_{13}}{G_{13}} \bar{l}_3 + 1} \qquad (13)$$

Knowing that $\bar{l}_1$ will affect G_{13} differently than, $\bar{l}_2$ $\bar{a}'_3$ can be thought of as $\vec{l}'_1$ $\vec{l}'_2$. Therefore, the analysis was completed by using only one void while holding $\bar{l}_1$ constant and varying $\bar{l}_2$. This was done
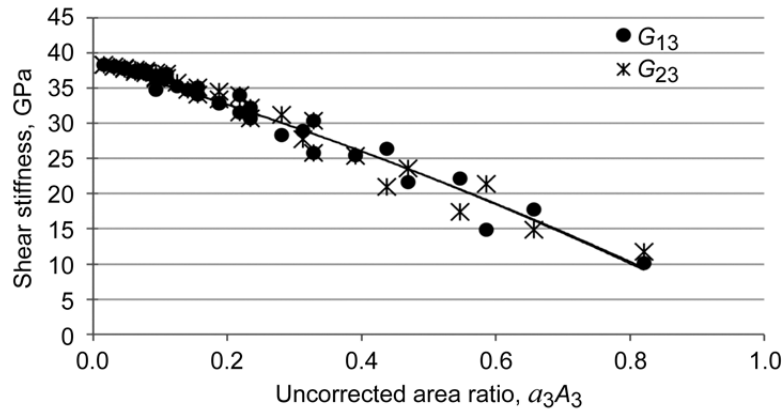
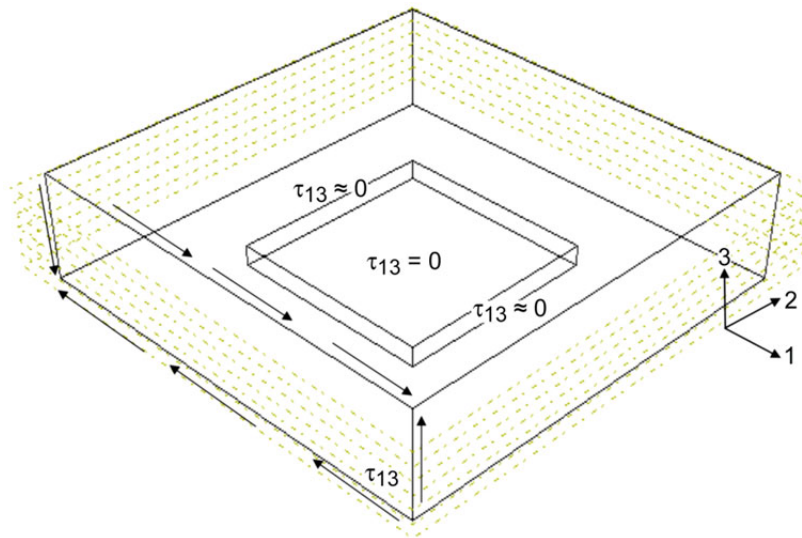Figure 18.—Area fraction of void versus shear stiffness.

Figure 19.—Shear stress around the void.

for several values of $\bar{l}'_1$. The data can be found in Table A3 of the Appendix. Similarly to the length correction in the previous section, a relationship between the actual area, $\bar{a}_3$ and the corrected area, $\bar{a}'_3$ can be found. The data are plotted in Figure 20. Through curve fitting, we found that the areas are related by the equation

$$\bar{a}'_3 = -1.84\bar{a}_3^2 + 2.60\bar{a}_3 \tag{14}$$

with an R^2 value of 0.97. The length fractions are plotted against the corrected area in Figure 21. For small l_1's, the effect of l_2 on the area is linear. As l_1 increases the relationship between l_2 and the corrected area becomes quadratic. This explains the deviation from linearity in the curve of Figure 20. The deviation from linearity between the uncorrected and corrected areas is likely caused by effects of the void approaching the boundary, as was observed in the transverse stiffness results.
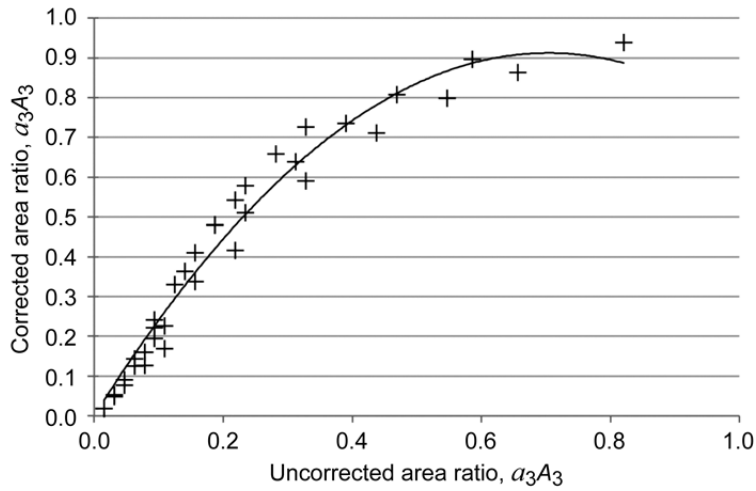
Figure 20.—Uncorrected area fraction versus corrected area fraction according to Equation (13).
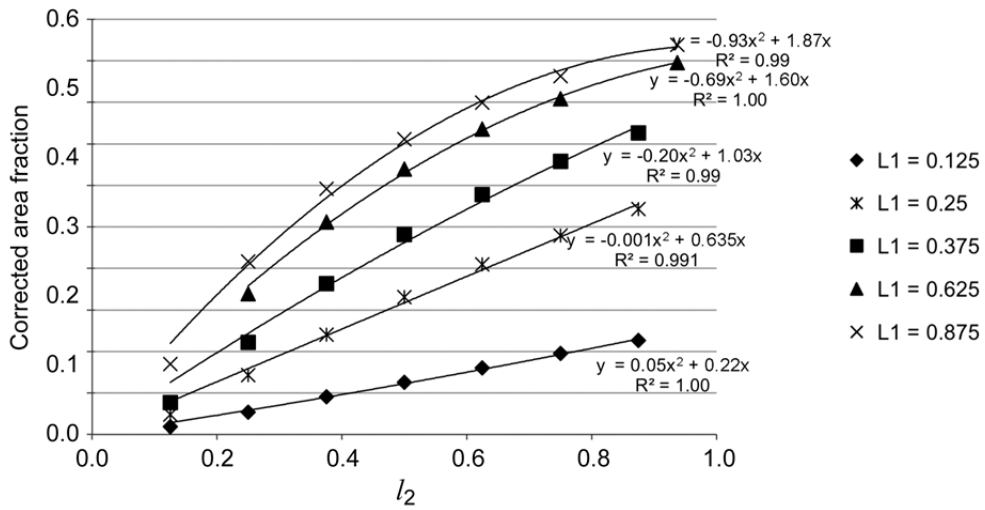

Figure 21.—Length fractions $\bar{l}_2$ and $\bar{l}_3$ versus the corrected area.

TABLE 6.—COMPARISON OF ΔG_{13} FOR SAMPLE CASES

	A_3	ΔG_{13} FEA, GPa	ΔG_{13} quadratic fit, GPa	ΔG_{13} corrected area, GPa
1 void	0.22	6.43	6.27	5.53
2 voids	0.27	5.78	8.07	5.48
3 voids	0.27	5.30	7.95	6.23
2 voids misaligned	0.23	4.74	6.81	5.76
4 voids, various AR	0.15	3.64	4.18	4.30
RMS error (GPa)	-----	-----	1.85	0.81

TABLE 7.—COMPARISON OF ΔG_{23} FOR SAMPLE CASES

	A_3	ΔG_{23} FEA, GPa	ΔG_{23} quadratic fit, GPa	ΔG_{23} corrected area, GPa
1 void	0.22	6.42	6.27	5.53
2 voids	0.27	7.36	8.07	5.48
3 voids	0.27	7.29	7.95	6.23
2 voids misaligned	0.23	6.14	6.81	5.76
4 voids, various AR	0.15	3.79	4.18	4.30
RMS error (GPa)	-----	-----	0.57	1.10

Tables 6 and 7 provide a comparison of the predicted decrease in shear stiffnesses for a few sample cases using Equation (11), for the quadratic fit to the projected area, and Equation (13), using the corrected area fraction calculated from the empirical relationship in Equation (14), versus the results from FEA. When comparing the results of the two tables, it is clear that G_{13} and G_{23} are not equivalent and likely dependent on some directional component that a relationship to area fraction cannot capture. It is not clear which method is more accurate. Further investigation regarding how the lengths, instead of only the area will be considered for future work.

6.0   Concluding Remarks

After completing finite element analysis on several cases of void size and spacing while the void volume fraction remained constant, it was clear that the voids affect the transverse stiffness and the out-of-plane shear stiffness the most (up to 15 percent stiffness degradation on average for a void volume fraction of 4 percent). In an attempt to determine the driving factors of the reduction in stiffness, we found that for the transverse stiffness, the projected area of the voids onto the 1-2 plane had a significant impact. A strong linear relationship was found between the area and the resulting stiffness, but the relationship involving a corrected length fraction provided a better physical understanding. The voids effect on the load bearing volume extends further than the space that the void occupies, which offers an explanation of why relationships based solely on volume fraction are not sufficient when the voids of the composite have large aspect ratios and are unevenly distributed. Similarly, we found that the shear stiffness is also related to the projected area of the voids onto the 1-2 plane. However, an area correction, rather than a length correction is most appropriate due to the small shear stress around the walls of the voids. Future work will consider the effects of non-symmetry in the shear stiffness. The problems that arise when there are more voids that are potentially overlapping will also be addressed.

Appendix—Effect of Void Geometry on Stiffness Properties

The void cases studied are described below and their respective data are found in Tables A1 and A2. The cases are shown pictorially in Section 3.0.

- 1 void; Centered; Aspect ratio (AR) = 3, AR = 5, AR = 8, AR = 10
- 2 voids; Centered and aligned in "1" direction; d1 constant; AR = 3, AR = 5, AR = 8, AR = 10
- 3 voids; Centered and aligned in "1" direction; d1 constant; AR = 3, AR = 5, AR = 8, AR = 10
- 2 voids; AR = 8; Aligned in "1" direction; s_1 = 0.15 mm, s_1 = 0.57 mm, s_1 = 1 mm, s_1 = 1.6 mm
- 2 voids; AR = 8; Aligned in "1" direction; s_1 constant; s_3—maximum possible distance apart (one void on bottom, one void on top)
- 2 voids; AR = 8; NOT aligned in "1" direction (located in opposite corners); s_1 constant; s_3—maximum possible distance apart (one void on bottom, one void on top);
- 3 voids; AR = 10; Voids diagonal, but in same plane
- 3 voids; AR = 10; Voids diagonal, but in different planes;

TABLE A1.—DATA FROM VOID CASES WITH VARYING ASPECT RATIOS

No. voids	AR	E_1, GPa	E_2, GPa	E_3, GPa	G_{12}, GPa	G_{13}, GPa	G_{23}, GPa
1	3	98.0	98.0	95.7	37.4	35.4	35.4
1	5	98.7	98.7	92.7	37.8	34.4	34.4
1	8	99.1	99.1	88.7	38.0	32.9	32.9
1	10	99.4	99.4	86.3	38.1	32.0	32.0
2	3	98.5	98.1	94.3	37.5	35.8	35.3
2	5	99.1	98.8	90.9	37.8	34.9	34.1
2	8	99.5	99.3	86.1	38.1	33.6	32.3
2	10	99.6	99.4	83.2	38.2	32.6	31.0
3	3	99.0	98.2	93.8	37.5	36.0	35.1
3	5	99.4	98.8	89.9	37.9	34.8	33.6
3	8	99.8	99.3	84.7	38.1	33.2	31.2
3	10	99.9	99.4	80.2	38.2	31.7	28.7

TABLE A2.—DATA FROM VOID CASES WITH ASPECT RATIO OF 8 AND VARYING SPATIAL DISTRIBUTIONS

No. voids	Spacing description	E_1, GPa	E_2, GPa	E_3, GPa	G_{12}, GPa	G_{13}, GPa	G_{23}, GPa
2	s_1 = 0.16 mm	99.6	99.3	86.0	38.1	33.0	31.7
2	s_1 = 0.57 mm	99.6	99.3	86.2	38.1	33.5	32.2
2	s_1 = 1 mm	99.5	99.3	86.2	38.1	33.6	32.3
2	s_1 = 1.6 mm	99.5	99.3	86.2	38.1	33.6	32.3
2	s_3 = max	99.5	99.3	86.0	38.1	33.7	32.3
2	Opposite corners	99.3	99.3	86.1	38.2	33.0	33.0
3	Diagonal; same plane	99.4	99.3	84.7	38.2	33.1	33.0
3	Diagonal; tiered planes	99.5	99.3	84.5	38.2	33.3	33.0

TABLE A3.—DATA FROM VOID CASES WITH 1 VOIDS AND CONSTANT VOID HEIGHT

l_1	l_2	E_1, GPa	E_2, GPa	E_3, GPa	G_{12}, GPa	G_{13}, GPa	E_1, GPa
0.001	0.001	99.9	99.9	99.5	38.4	38.3	38.3
0.001	0.002	99.8	99.9	98.8	38.4	38.1	38.1
0.001	0.003	99.7	99.9	98.1	38.4	37.8	37.9
0.001	0.004	99.5	99.9	97.4	38.3	37.5	37.7
0.001	0.005	99.4	99.9	96.6	38.3	37.1	37.5
0.001	0.006	99.3	99.9	95.9	38.2	36.8	37.2
0.001	0.007	99.1	99.9	95.2	38.2	36.5	37.1
0.002	0.001	99.9	99.8	98.8	38.4	38.1	38.1
0.002	0.002	99.7	99.7	96.9	38.3	37.3	37.3
0.002	0.003	99.6	99.7	94.9	38.3	36.3	36.5
0.002	0.004	99.4	99.7	93.0	38.2	35.2	35.8
0.002	0.005	99.3	99.7	90.9	38.2	34.1	35.1
0.002	0.006	99.1	99.8	88.9	38.1	32.9	34.5
0.002	0.007	98.9	99.8	86.8	38.1	31.5	34.0
0.003	0.001	99.9	99.7	98.1	38.4	37.9	37.8
0.003	0.002	99.7	99.6	95.0	38.3	34.8	36.3
0.003	0.003	99.5	99.5	91.7	38.2	34.8	34.8
0.003	0.004	99.4	99.5	88.4	38.2	32.8	33.4
0.003	0.005	99.2	99.6	85.1	38.1	30.7	32.2
0.003	0.006	99.0	99.6	81.6	38.0	28.4	31.2
0.003	0.007	98.8	99.7	78.1	38.0	25.8	30.3
0.005	0.001	99.9	99.4	96.7	38.3	37.5	37.1
0.005	0.002	99.7	99.3	90.9	38.2	35.1	34.1
0.005	0.003	99.6	99.2	85.1	38.1	32.2	30.7
0.005	0.004	99.4	99.2	78.9	38.0	29.0	27.7
0.005	0.005	99.2	99.2	72.5	38.0	25.4	25.4
0.005	0.006	99.0	99.3	65.8	37.9	21.6	23.6
0.005	0.0075	98.7	99.7	55.3	37.9	14.9	21.4
0.007	0.001	99.9	99.1	95.2	38.2	37.1	36.5
0.007	0.002	99.8	98.9	86.8	38.1	34.0	31.5
0.007	0.003	99.7	98.8	78.1	38.0	30.3	25.8
0.007	0.004	99.6	98.8	68.8	37.9	26.4	21.0
0.007	0.005	99.5	98.8	58.9	37.9	22.2	17.4
0.007	0.006	99.4	99.0	48.4	37.9	17.7	14.8
0.007	0.0075	99.2	99.5	31.5	38.0	10.1	11.8

References

1. Ohnabe, H., Masaki, S., Onozuka, M., Miyahara, K., and Sasa, T., "Potential application of ceramic matrix composites to aero-engine components," *Composites Part A: Applied Science and Manufacturing*, vol. 30, Apr. 1999, pp. 489–496.
2. Goldsmith, M.B., Sankar, B.V, Haftka, R.T., and Goldberg, R.K., "Effects of Microstructural Variability on Thermo-Mechanical Properties of a Woven Ceramic Matrix Composite," NASA/TM—2013-217817, 2013.
3. Madsen, B., and Lilholt, H., "Physical and mechanical properties of unidirectional plant fibre composites—an evaluation of the influence of porosity," *Composites Science and Technology*, vol. 63, Jul. 2003, pp. 1265–1272.
4. Pal, R., "Porosity-dependence of Effective Mechanical Properties of Pore-solid Composite Materials," *Journal of Composite Materials*, vol. 39, Jul. 2005, pp. 1147–1158.
5. Peters, P., Martin, E., and Pluvinage, P., "Influence of porosity and fibre coating on engineering elastic moduli of fibre-reinforced ceramics (SiC/SiC)," *Composites*, vol. 26, 1995, pp. 108–114.
6. Wu, Y., Shivpuri, R., and Lee, L.J., "Effect of Macro and micro Voids on Elastic Properties of Polymer Composites," *Journal of Reinforced Plastics and Composites*, vol. 17, 1998.
7. Tsukrov, I., and Kachanov, M., "Effective moduli of an anisotropic material with elliptical holes of arbitrary orientational distribution," *International Journal of Solids and Structures*, vol. 37, 2000, pp. 5919–5941.
8. Huang, H., and Talreja, R., "Effects of void geometry on elastic properties of unidirectional fiber reinforced composites," *Composites Science and Technology*, vol. 65, Oct. 2005, pp. 1964–1981.
9. Goldberg, R.K., Bonacuse, P.J., and Mital, S.K., "Investigation of Effects of Material Architecture on the Elastic Response of a Woven Ceramic Matrix Composite," NASA/TM—2012-217269, 2012.
10. "ABAQUS Software Package, Ver. 6.8, SIMULIA, Providence, RI."

1. REPORT DATE (DD-MM-YYYY) 01-06-2013	2. REPORT TYPE Technical Memorandum	3. DATES COVERED (From - To)

4. TITLE AND SUBTITLE
Quantifying Effects of Voids in Woven Ceramic Matrix Composites

5a. CONTRACT NUMBER

5b. GRANT NUMBER

5c. PROGRAM ELEMENT NUMBER

6. AUTHOR(S)
Goldsmith, Marlana, B.; Sankar, Bhavani, V.; Haftka, Raphael, T.; Goldberg, Robert, K.

5d. PROJECT NUMBER

5e. TASK NUMBER

5f. WORK UNIT NUMBER
WBS 794072.02.03.03.03

7. PERFORMING ORGANIZATION NAME(S) AND ADDRESS(ES)
National Aeronautics and Space Administration
John H. Glenn Research Center at Lewis Field
Cleveland, Ohio 44135-3191

8. PERFORMING ORGANIZATION REPORT NUMBER
E-18673

9. SPONSORING/MONITORING AGENCY NAME(S) AND ADDRESS(ES)
National Aeronautics and Space Administration
Washington, DC 20546-0001

10. SPONSORING/MONITOR'S ACRONYM(S)
NASA

11. SPONSORING/MONITORING REPORT NUMBER
NASA/TM-2013-217874

12. DISTRIBUTION/AVAILABILITY STATEMENT
Unclassified-Unlimited
Subject Categories: 24 and 39
Available electronically at http://www.sti.nasa.gov
This publication is available from the NASA Center for AeroSpace Information, 443-757-5802

13. SUPPLEMENTARY NOTES

14. ABSTRACT
Randomness in woven ceramic matrix composite architecture has been found to cause large variability in stiffness and strength. The inherent voids are an aspect of the architecture that may cause a significant portion of the variability. A study is undertaken to investigate the effects of many voids of random sizes and distributions. Response surface approximations were formulated based on void parameters such as area and length fractions to provide an estimate of the effective stiffness. Obtaining quantitative relationships between the properties of the voids and their effects on stiffness of ceramic matrix composites are of ultimate interest, but the exploratory study presented here starts by first modeling the effects of voids on an isotropic material. Several cases with varying void parameters were modeled which resulted in a large amount of variability of the transverse stiffness and out-of-plane shear stiffness. An investigation into a physical explanation for the stiffness degradation led to the observation that the voids need to be treated as an entity that reduces load bearing capabilities in a space larger than what the void directly occupies through a corrected length fraction or area fraction. This provides explanation as to why void volume fraction is not the only important factor to consider when computing loss of stiffness.

15. SUBJECT TERMS
Ceramic matrix composites; Micromechanics

16. SECURITY CLASSIFICATION OF:			17. LIMITATION OF ABSTRACT	18. NUMBER OF PAGES	19a. NAME OF RESPONSIBLE PERSON STI Help Desk (email:help@sti.nasa.gov)
a. REPORT U	b. ABSTRACT U	c. THIS PAGE U	UU	24	19b. TELEPHONE NUMBER (include area code) 443-757-5802